2487

Submitted to Applied Physics Letters (Sep 2002)

Structuring of sapphire by sequential He^+ ion-beam implantation and wet chemical etching

A. Crunteanu*, G. Jänchen, P. Hoffmann, and M. Pollnau

Institute of Imaging and Applied Optics, Swiss Federal Institute of Technology,

CH-1015 Lausanne, Switzerland

Ch. Buchal and A. Petraru

Institut für Schichten und Grenzflächen, ISG-IT, Forschungszentrum Jülich,

D-52425 Jülich, Germany

R.W. Eason and D.P. Shepherd

Optoelectronics Research Centre, University of Southampton,

Highfield, Southampton SO17 1BJ, United Kingdom

*Corresponding author.

Fax +41-21-6933701; e-mail: aurelian.crunteanustanescu@epfl.ch

Abstract

We present a method for the selective two- and three-dimensional patterning of sapphire: light ion-beam implantation to generate severe lattice damage to depths exceeding 1 µm and subsequent selective wet chemical etching of the damaged regions by hot H_3PO_4. C-cut sapphire crystals were implanted through contact masks using ion fluences of $1x10^{16}$ to $5x10^{17}$ He^+/cm^2 and energies up to 400 keV. The etching process is characterized by a high selectivity and a rate of ~19 nm/min. Whereas an implantation that produces a continuously damaged pathway results in complete etching from the surface, sole in-depth implantation using only high-energy ions leads to under-etching of the crystalline surface layer. By a combination of these processes we have fabricated three-dimensional structures such as channels and bridges in sapphire.

PACS numbers:

81.65.Cf, 79.20.Rf, 41.75.Ak

Three-dimensional (3D) microstructures that are of interest for many applications have been fabricated in a number of materials and by a number of different processes. For example, structures like V-grooves in silicon or $LiNbO_3$ [1] were formed by anisotropic wet chemical etching. 3D microstructures for MEMS devices were fabricated by serial processing in positive (PMMA) or negative (SU8) resists using techniques such as light-induced spatially resolved two-photon polymerization [2] or deep ion-beam lithography (DIBL) with MeV protons [3]. 3D channels were fabricated in quartz using a Q-switched Nd:YAG laser [4]. 3D structures were demonstrated in GaAs using nitrogen implantation at MeV energies [5]. Low-dose He^+ implantation has been applied to in-depth modifications of optical materials for waveguide fabrication [6, 7] and for slicing freestanding μm-thick samples of crystalline materials such as $LiNbO_3$ [8].

Sapphire is an insulator that exhibits high chemical and thermal stability. It is used for the isolation of microelectronic structures and as a dielectric substrate for electronic and optoelectronic devices in the silicon-on-sapphire technology. The patterning of sapphire films for the fabrication of microelectronic, optoelectronic, or micro-electromechanical systems (MEMS) is difficult, since conventional chemical etching procedures are not applicable. Alternative methods such as Ar^+ milling, plasma etching, or reactive ion etching have been applied successfully but are limited to structures that permit a direct ballistic access of the active agents. To our knowledge, 3D structures in sapphire have as yet not been reported.

We demonstrate a new way for the 3D structuring of sapphire. In a first step, ion implantation is used to tailor an appropriate damage profile within the crystal. In a second step, wet chemical etching is performed to selectively remove the damaged material. Ion implantation of sapphire produces damage clusters and, depending on

ion type, dose and energy, even complete amorphization of implanted regions [6, 9]. Recent studies [10-13] have shown that amorphous Al_2O_3 produced by implantation with heavy ions of different energies (55-180 keV) and fluences ($3x10^{15}$-$9x10^{17}$ ions/cm^2) can be attacked by several chemical etchants while the crystalline material is not affected. A high etching rate of ~16 nm/min was obtained with phosphoric acid (H_3PO_4) [14]. However, the use of heavy ions of moderate energies of a few hundred keV permits the structuring of sapphire for depths of only a few hundreds of nanometers and the generated damage always includes the surface region.

The implantation of light ions such as H^+ and He^+ into sapphire allows for deeper damage profiles exceeding 1 μm and for in-depth amorphization without significant damage of the surface region. We tailored damage profiles into the sapphire substrates by masking regions (for example in the form of stripes) that were not exposed to ion implantation. Since wire-type proximity masks impair the resolution and edge quality between the implanted and non-implanted areas, we used lithographically patterned contact-resist masks with a thickness of 1.8 μm. After ion implantation, the masks were removed and the samples were etched in a bath of 85% H_3PO_4 at 165°C for varying times. At higher temperatures, H_3PO_4 dehydrates and condenses from ortho-phosphoric to a mixture of ortho-, pyro-, or higher poly-phosphoric acids [15]. The etching depths and the structures obtained were investigated using profilometry measurements, optical microscopy, scanning electron microscopy (SEM), and atomic force microscopy (AFM).

Firstly, we investigated in detail the influence of the implantation conditions on the etching behavior of sapphire by varying the He^+ energy and implantation doses. Table I presents the experimental implantation conditions for four representative samples (A to D). The damage induced by the He^+ ions was simulated

using the SRIM-2000.40 package [16]. The calculated results should be considered as a qualitative guideline only, because possible recombination processes as well as the influence of the increasing lattice disorder during the irradiation process are not included in this computer code. Figure 1 displays the damage profiles induced by the different ion energies as well as the accumulated damage profiles generated in each sample presented in Table I. The figure shows that for a given energy, the major damage is confined to a region at the end of the ion range. The depth of the buried damaged layer depends on the ion energy, while the amount of damage (the height of the damage peak) is defined by the implantation dose.

Sample A was implanted using only the maximum energy of 400 keV at a total fluence of $5x10^{17}$ ions/cm^2. According to the simulations, implantation of sapphire with 400-keV He^+ ions results in a buried damaged layer ~1.1-1.2 μm below the surface (Fig. 1, curve 1). Under these conditions, the surface remained almost non-damaged and no visible change of the surface was observed even after 80 h of etching. Etching of the damaged layer occurred from the side. Evidently, in order to achieve etching from the surface down, a continuously damaged pathway must be produced that extends from the surface of the sample down to the desired depth.

To achieve a continuous damage profile, He^+ implantation was undertaken for sample B using a set of five energies (400, 290, 190, 110, and 50 keV) with a total implantation fluence of $5x10^{17}$ ions/cm^2. The SRIM estimation of the accumulated damage profile (Fig. 1, curve 2) is continuous inside the sapphire, although the damage level is significantly lower in the immediate vicinity of the surface. Etching of sample B for 18 min. resulted in structures of a height of ~350 nm, as measured by profilometry. This suggests an etching rate of ~19 nm/min.

Further etching of the sample removed the implanted regions to a depth of 1.2 μm, but parts of the non-implanted lines were then also removed. We suppose that the partial removal of material at the surface of the non-implanted regions is due to the under-etching of the less damaged implanted surface layer followed by mechanical stress and breakage of this layer, which damages also the non-implanted regions and allows subsequent acid attack. This result implies that on the one hand, the production of well-defined structures requires a higher implantation dose also in the vicinity of the surface, whereas on the other hand, under-etching to produce 3D buried structures requires a non-damaged crystalline surface layer of larger thickness in order to avoid breakage.

In order to improve the onset of etching and simultaneously avoid under-etching and breakage, two samples (C and D) were consecutively implanted with ion energies of 290, 190, 110, 50, and 25 keV. The envelope of the accumulated damage profile is presented in Fig. 1 (curve 3). It can be seen that by adding the ion implantation energy of 25 keV, the damage profile extends nearer towards the sample surface. In order to investigate the influence of the implantation dose, samples C and D were implanted with fluences of $1x10^{16}$ and $1x10^{17}$ ions/cm^2, respectively, for each energy.

We did not observe any modification on the surface of sample C even after several hours of etching. This implies the existence of an implantation-dose threshold for sufficient damage or amorphization of sapphire to permit the onset of etching, as was suggested also in Ref. [6]. Etching of sample D resulted in ribs (corresponding to the non-implanted regions) with heights of up to 1.1 μm. Figure 2 shows a contact-mode AFM 3D profile of such a rib obtained after 30 min of etching. The rib surface possesses a relatively low rms roughness of ~21 nm. SEM

investigations showed that the ribs are characterized by well-defined and sharp edges, with a step slope of ~78°. Most important, etching experiments conducted for more than 20 h showed that the ribs are not attacked by the acid, proving the high etching selectivity between implanted and non-implanted sapphire.

Finally, we performed 3D structuring of sapphire by sequential implantation through two 50-μm thick molybdenum contact masks. Larger regions of a sapphire substrate were implanted through a first mask using high He^+ energies of 290 and 190 keV. Parts of these pre-implanted regions were further irradiated through a second mask using lower He^+ energies of 110, 50, and 25 keV. The ion fluences were $1x10^{17}$ ions/cm^2 for each energy. In this way, we created regions with a continuous damage profile up to the sample surface that were adjacent to regions with a buried damaged layer. By etching in H_3PO_4 we obtained 3D structures in sapphire (see Fig. 3) with under-etched buried regions of up to 80x30 μm^2 in size underneath a non-damaged surface layer.

This process is currently limited by the highest He^+ energy available in our experiment, which defines the maximum implantation depth of ~1.1 μm and leads to a ~500-nm thin surface layer that tends to be fragile. The use of higher implantation energies, which will lead to larger implantation depths of a few micrometers and allow for a thicker, more stable surface layer, will overcome this problem.

We conclude that He^+ implantation followed by H_3PO_4 wet chemical etching is an appropriate method for micro-structuring sapphire. It allows for etching depths of more than 1 μm while preserving a high etching selectivity between the implanted and non-implanted regions. A continuous damage profile of the implanted regions up to the sample surface is required to obtain well-defined structures. This etching method can be applied to the fabrication of optical rib waveguides in sapphire or

Ti:sapphire as well as more complex features like directional or branching waveguide couplers. In addition, by use of different combinations of masks, implantation energies and doses, this method permits the fabrication of complex 3D structures inside sapphire crystals with undercut or re-entrant features. This possibility represents a significant advantage over other structuring methods. Applications may include undercutting and ion slicing for isolating sapphire thin films for sensor applications in silicon-on-sapphire technology or complex micro-fluidic channels in sapphire for high-temperature applications.

This work was partially supported by the Swiss National Science Foundation.

References

[1] R.W. Eason, I.E. Barry, G.W. Ross, and P.G.R. Smith, Electron. Lett **35**, 328 (1999).

[2] S. Kawata, H.B. Sun, T. Tanaka, and K. Takada, Nature **412**, 697 (2001).

[3] J.A. van Kan, J.L. Sanchez, B. Xu, T. Osipowicz, and F. Watt, Nucl. Instrum. Methods B **148**, 1085 (1999).

[4] S.-J. Qin and W.J. Li, Appl. Phys. A **74**, 773 (2002).

[5] J. Miao, I.M. Tiginyanu, H.L. Hartnagel, G. Irmer, J. Monecke, and B.L. Weiss, Appl. Phys. Lett. **70**, 847 (1997).

[6] P.D. Townsend, P.J. Chandler, and L. Zhang, *Optical Effects of Ion Implantation* (Cambridge University Press, Cambridge, 1994).

[7] Ch. Buchal, S.P. Withrow, C.W. White, and D.B. Poker, Annu. Rev. Mater. Sci. **24**, 125 (1994).

[8] T. Ramadan, M. Levy, and R.M. Osgood, Jr., Appl. Phys. Lett. **76**, 1407 (2000).

[9] C.W. White, C.J. McHargue, P.S. Skland, L.A. Boatner, and G.C. Farlow, Mater. Sci. Rep. **4**, 41 (1989).

[10] M. Ishida, H. Kim, T. Kimura, and T. Nakamura, Sensor Actuat. A-Phys. **53**, 340 (1996).

[11] C.J. McHargue, J.D. Hunn, D.L. Joslin, E. Alves, M.F. da Silva, and J.C. Soares, Nucl. Instrum. Methods B **127/128**, 596 (1997).

[12] P. Levy, S. Nicoletti, L. Correra, M. Cervera, M. Bianconi, F. Biscarini, F. Corticelli, and E. Gabilli, Nuovo Cimento D **19**, 1389 (1997).

[13] D. Xie, D. Zhu, H. Pan, H. Xu, and Z. Ren, J. Phys. D: Appl. Phys. **31**, 1647 (1998).

[14] E. Makino, T. Shibata, and Y. Yamada, Sensor Actuat. A-Phys. **75**, 278 (1999).

[15] S. Ohashi and H. Sugatani, B. Chem. Soc. Jpn. **30**, 864 (1957).

[16] SRIM-2000, "The Stopping and Range of Ions in Matter" package at www.srim.org.

Table I. He^+ implantation parameters and projected depth ranges for samples A to D

Implantation energy (keV)	Projected range (μm)	Straggling (μm)	Implantation fluence (He^+ cm^{-2}) Sample A	B	C	D
25	0.17	± 0.07	-	-	1×10^{16}	1×10^{17}
50	0.30	± 0.09	-	1×10^{17}	1×10^{16}	1×10^{17}
110	0.50	± 0.10	-	1×10^{17}	1×10^{16}	1×10^{17}
190	0.74	± 0.11	-	1×10^{17}	1×10^{16}	1×10^{17}
290	0.97	± 0.12	-	1×10^{17}	1×10^{16}	1×10^{17}
400	1.21	± 0.12	5×10^{17}	1×10^{17}	-	-
Total fluence (He^+ cm^{-2})			5×10^{17}	5×10^{17}	5×10^{16}	5×10^{17}

Figure Captions

Fig. 1. Simulated damage profiles within sapphire generated by He^+ ions with different energies (displayed as number of vacancies generated per incident ion per Å depth). Accumulated damage profiles: curve 1 corresponds to sample A, 2 to sample B, and 3 to samples C and D.

Fig. 2. Contact-mode AFM 3D image of a rib structure obtained after 30 min etching of sample D

Fig. 3. SEM image of an under-etched region in sapphire

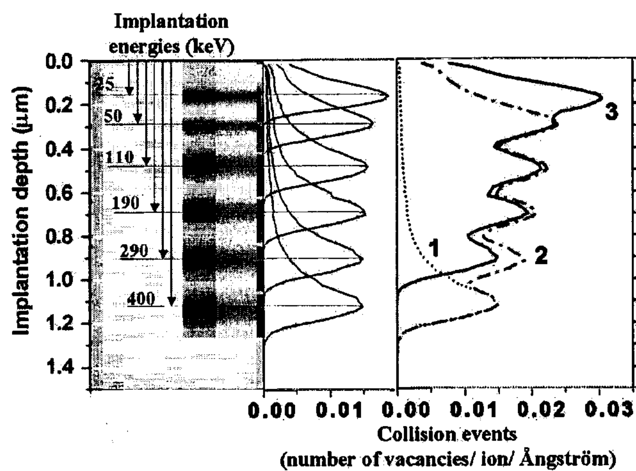
Implantation energies (keV)
25
50
110
190
290
400
Implantation depth (µm)
0.0
0.2
0.4
0.6
0.8
1.0
1.2
1.4
1
2
3
0.00 0.01 0.00 0.01 0.02 0.03
Collision events
(number of vacancies/ ion/ Ångström)

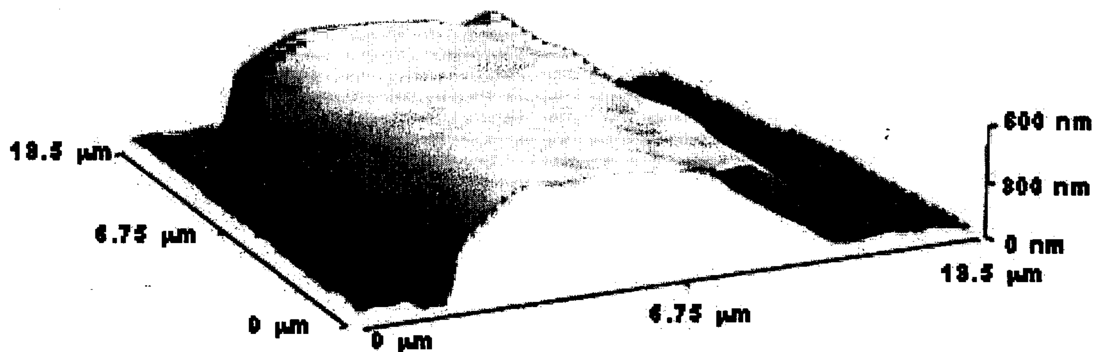
13.5 µm
6.75 µm
0 µm
0 µm
6.75 µm
13.5 µm
600 nm
300 nm
0 nm

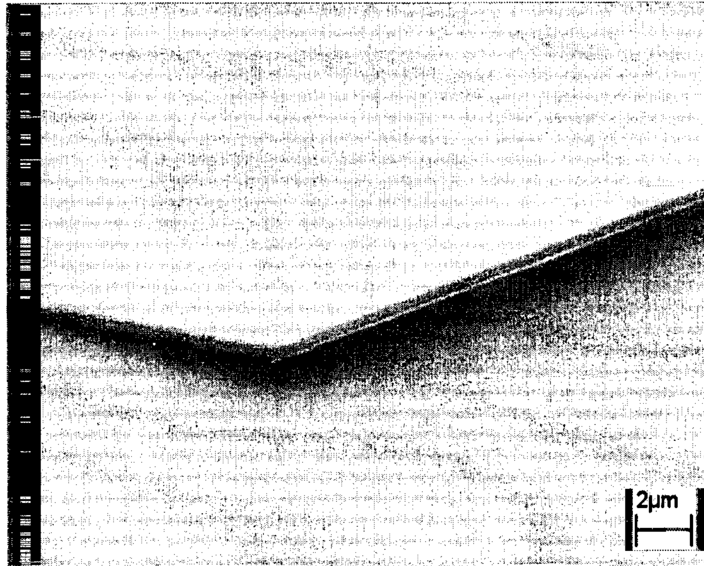
2µm